Available online at www.sciencedirect.com
ScienceDirect
Journal of Power Sources 163 (2007) 846–852
JOURNAL OF POWER SOURCES
www.elsevier.com/locate/jpowsour

A fractal model for predicting permeability and liquid water relative permeability in the gas diffusion layer (GDL) of PEMFCs

Guangli He [a], Zongchang Zhao [a,*], Pingwen Ming [b], Abudula Abuliti [c], Caoyong Yin [a]

[a] *School of Chemical Engineering, Dalian University of Technology, Dalian 116012, PR China*
[b] *Fuel Cell R&D Center, Dalian Institute of Chemical Physics, Chinese Academy of Sciences, Dalian 116023, PR China*
[c] *New Energy Technology Research Division, Aomori Industrial Research Center, Aomori 030-0113, Japan*

Received 19 July 2006; received in revised form 24 September 2006; accepted 26 September 2006
Available online 13 November 2006

Abstract

In this study, a fractal model is developed to predict the permeability and liquid water relative permeability of the GDL (TGP-H-120 carbon paper) in proton exchange membrane fuel cells (PEMFCs), based on the micrographs (by SEM, i.e. scanning electron microscope) of the TGP-H-120. Pore size distribution (PSD), maximum pore size, porosity, diameter of the carbon fiber, pore tortuosity, area dimension, hydrophilicity or hydrophobicity, the thickness of GDL and saturation are involved in this model. The model was validated by comparison between the predicted results and experimental data. The results indicate that the water relative permeability in the hydrophobicity case is much higher than in the hydrophilicity case. So, a hydrophobic carbon paper is preferred for efficient removal of liquid water from the cathode of PEMFCs.

Keywords: Fractal model; Relative permeability; Gas diffusion layer (GDL); PEMFC; Fuel cell

1. Introduction

Carbon paper is commonly used as the gas diffusion layer (GDL) in the application of PEMFCs, which is composed of randomly packed carbon fibers. The GDL is an important part of PEMFCs. It has several functions: reactant permeability, product permeability (i.e. liquid water removal), electronic conductivity, heat conductivity and mechanical strength for providing mechanical support to the MEA. The properties of the GDL directly influence the performance of PEMFCs [1–5], which are determined by the GDL's microstructure. However, there are only a few reports on the relationship between the GDL's properties and microstructure. Newman and co-workers [6] developed a statistical method for predicting the pore size distribution (PSD), permeability and capillary pressure in a GDL. In the present work, a fractal model is developed for predicting the absolute permeability and water relative permeability based on the microstructure of the GDL obtained by SEM. Pore size distribution, maximum pore size, porosity, diameter of the carbon fiber, pore tortuosity, area dimension, hydrophilicity or hydrophobicity, and the thickness of GDL as well as saturation are involved in this model, which provides an insight into the properties of the GDL and the water management in PEMFCs.

2. Fractal theory

Euclidean geometry describes ordered objects using integer dimensions 0, 1, 2 and 3, respectively. However, numerous objects found in Nature [7] such as rough surfaces, coastlines, mountains, and islands, are disordered and irregular, and they do not follow the Euclidean description since their length, area and volume are scale-dependent [8]. Such objects are called fractals, and are described using a non-integral dimension called the fractal dimension [8]. The measure of a fractal structure, $M(L)$ is related to the length scale, L, through a power law in the form of [7]:

$$M(L) \; L^{D_f} \tag{1}$$

where '$\sim$' means 'scales as', and D_f is the fractal dimension of the structure. Associated with Eq. (1), the property of self-similarity implies that the value of D_f calculated from the rela-

* Corresponding author. Tel.: +86 411 88993626.
E-mail address: zczhao55@163.com (Z. Zhao).

0378-7753/$ – see front matter © 2006 Elsevier B.V. All rights reserved.
doi:10.1016/j.jpowsour.2006.09.054

Nomenclature

A_0	unit area (cm^2)
d	fiber diameter (μm)
d_t	tortuosity dimension
D_f	area dimension
f_{HI}	fraction of hydrophilic pores
K	permeability (cm^2)
l_s	length of space (cm)
L_0	straight length (cm)
p	pressure
q	flow rate in a capillary
Q	total flow rate
s	saturation

Greek letters

ε	porosity
θ	contact angle
λ	pore diameter (cm)
σ	surface tension

Subscripts

c	critical
cap	of capillary
max	maximum
min	minimum
rw	of water relative
rwi	of water relative for hydrophilicity case
rwo	of water relative for hydrophobicity case

tionship in Eq. (1) remains constant over a range of length scales, L. Geometric constructs such as the Sierpinsky gasket and the Koch curve are the examples of exact fractals which exhibit identical self-similarity over an infinite range of length scales. However, self-similarity in a global sense is seldom observed in nature and the fractal description is based on a statistical self-similarity, i.e. the objects exhibit self-similarity in some average sense, over a certain local range of length scale, L, relevant to the problem [9]. The concept of statistical self-similarity introduced above is used in the following section to develop a geometric description of the GDL in PEMFCs.

2.1. Fractal characteristics of GDL

Carbon paper is mainly used as the GDL of PEMFCs, which is composed of randomly packed carbon fibers [10]. It has numerous pores with various sizes in the through-plane direction, and can be considered as a bundle of tortuous capillary tubes with variable radius for the two-dimensional case. Let the diameter of a capillary tube in GDL be λ, and its tortuous length along the flow direction be $L(\lambda)$. The relationship between them also exhibits the fractal scaling law [11]:

$$\frac{L(\lambda)}{L_0} = \left(\frac{L_0}{\lambda}\right)^{d_t-1} \tag{2}$$

where L_0 is the representative length of a straight capillary, and d_t is the tortuosity dimension, with $1 \le d_t \le 2$. Large value of d_t within this range corresponds to a highly tortuous capillary, while $d_t = 1$ denotes a straight capillary pathway, $d_t = 2$, corresponds to a highly tortuous line that fills a plane [12].

Besides the convolutedness of the capillary pathways, the relationship between the number of pores and the pore size λ is another important property. The pores in a porous medium are analogous to the islands or lakes on the earth [13]. The cumulative size distribution of them follows the power law relation [13]:

$$N(L \ge \lambda) = \left(\frac{\lambda_{max}}{\lambda}\right)^{D_f} \tag{3}$$

where $N(L \ge \lambda)$ represents the total number of pores with diameter greater than λ, λ_{max} is the maximum pore diameter. From Eq. (3), the total pore number can be obtained

$$N_t(L \ge \lambda_{min}) = \left(\frac{\lambda_{max}}{\lambda_{min}}\right)^{D_f} \tag{4}$$

and

$$-dN = D_f \lambda_{max}^{D_f} \lambda^{-(D_f+1)}\, d\lambda \tag{5}$$

The negative sign in Eq. (5) implies that the pore population decreases with the increase of pore size, and $dN > 0$. Eqs. (1) and (3) hold true for both exactly and statistically self-similar fractal geometries. Here, $1 \le D_f \le 2$, for two-dimensional space. According to Eqs. (4) and (5):

$$-\frac{dN}{N_t} = D_f \lambda_{min}^{D_f} \lambda^{-(D_f+1)}\, d\lambda = f(\lambda)\, d\lambda \tag{6}$$

where $f(\lambda)$ is the probability density function, and

$$\int_{-\infty}^{\infty} f(\lambda)\, d\lambda = \int_{\lambda_{min}}^{\lambda_{max}} f(\lambda)\, d\lambda = 1 - \left(\frac{\lambda_{min}}{\lambda_{max}}\right)^{D_f} \tag{7}$$

The above equation equals unity if and only if

$$\frac{\lambda_{min}}{\lambda_{max}} = 0 \tag{8}$$

It implies that $\lambda_{min} \ll \lambda_{max}$ must be satisfied for fractal analysis of a porous media, otherwise the porous media is a non-fractal medium. As for the GDL of PEMFCs, it holds true according to the measured pore size distribution [10], so it is a fractal.

2.2. Fractal model for permeability of GDL

The total volumetric flow rate, Q, through a unit cell is a sum of the flow rates through all the individual capillaries. The flow rate through a single tortuous capillary is given by modifying the well-known Hagen–Poiseulle equation [14] to give

$$q(\lambda) = \frac{\pi}{128} \frac{\Delta p}{L(\lambda)} \frac{\lambda^4}{\mu} \tag{9}$$

Then, the total volumetric flow rate in a unit cell is

$$Q = -\int_{\lambda_{min}}^{\lambda_{max}} q(\lambda)\, dN(\lambda) \tag{10}$$

The permeability can be expressed as follows according to the Dacy's law:

$$k = \frac{\mu L_0 Q}{\Delta p A_0} = \frac{\pi}{128}\lambda_{\max}^{3+d_t} L_0^{-1-d_t} D_f \frac{1-(\lambda_{\min}/\lambda_{\max})^{3+d_t-D_f}}{3+d_t-D_f}$$

$$= \frac{\pi}{128}\lambda_{\max}^{3+d_t} L_0^{-1-d_t} D_f \frac{1}{3+d_t-D_f} \quad (11)$$

where $A_0 = L_0^2$ is the unit area.

Thus, Eq. (11) gives the absolute permeability of carbon paper obtained by the fractal theory, and the maximum pore size (λ_{max}), the thickness of the carbon paper ($L_0 = 0.037$ cm [15] for TGP-H-120), the tortuosity dimension (d_t), and the area dimension (D_f) are involved.

2.3. Fractal model for water relative permeability of GDL

Capillary-driven liquid water behavior in GDL is related to the wetting property of GDL for the two-phase flow situation. First, for hydrophilicity case, water transports by wicking function, and the capillary force can be calculated as $p_{cap} = 4\sigma\cos(\theta)/\lambda_c$, so the wicking function increases while pore size decreases. It means that water prior to transports through the small pores and the critical pore diameter λ_c (i.e. the maximum size of the pore that water can flow through) increases as saturation increases. The relationship between critical diameter and saturation is

$$s = \frac{\int_{\lambda_{\min}}^{\lambda_c} \lambda^2 D_f \lambda_{\min}^{D_f} \lambda^{-D_f-1}\,d\lambda}{\int_{\lambda_{\min}}^{\lambda_{\max}} \lambda^2 D_f \lambda_{\min}^{D_f} \lambda^{-D_f-1}\,d\lambda} \quad (12)$$

According to Eqs. (10) and (11), the water relative permeability can be determined as

$$k_{rwi} = \frac{\mu L_0 Q_W/\Delta p A_0}{\mu L_0 Q/\Delta p A_0} = \frac{Q_W}{Q} = \frac{\int_{\lambda_{\min}}^{\lambda_c} q(\lambda)\,dN(\lambda)}{\int_{\lambda_{\min}}^{\lambda_{\max}} q(\lambda)\,dN(\lambda)} \quad (13)$$

Submitting Eqs. (5), (8) and (9) into the equation above, then

$$k_{rwi} = \frac{\lambda_c^{3+d_t-D_f} - \lambda_{\min}^{3+d_t-D_f}}{\lambda_{\max}^{3+d_t-D_f} - \lambda_{\min}^{3+d_t-D_f}} = \left(\frac{\lambda_c}{\lambda_{\max}}\right)^{3+d_t-D_f} \quad (14)$$

Eq. (14) is the final expression for liquid water relative permeability of the GDL for the hydrophilicity case, where λ_c can be obtained in Eq. (12).

As for the hydrophobicity case, initial pressure is needed for water transport due to the hydrophobicity, which can also be calculated as $p_{cap} = 4\sigma\cos(\theta)/\lambda_c$. It means the lager pores need smaller initial pressure. Water prefers moving through large pores, and the critical pore size (i.e. the minimum size of the pore that water can flood) decreases as saturation increases, so the saturation can be determined as

$$s = \frac{\int_{\lambda_c}^{\lambda_{\max}} \lambda^2 D_f \lambda_{\min}^{D_f} \lambda^{-D_f-1}\,d\lambda}{\int_{\lambda_{\min}}^{\lambda_{\max}} \lambda^2 D_f \lambda_{\min}^{D_f} \lambda^{-D_f-1}\,d\lambda} \quad (15)$$

The water relative permeability is

$$k_{rwo} = \frac{\mu L_0 Q_W/\Delta p A_0}{\mu L_0 Q/\Delta p A_0} = \frac{Q_W}{Q} = \frac{\int_{\lambda_c}^{\lambda_{\max}} q(\lambda)\,dN(\lambda)}{\int_{\lambda_{\min}}^{\lambda_{\max}} q(\lambda)\,dN(\lambda)} \quad (16)$$

Submitting Eqs. (5), (8) and (9) into equation above, then

$$k_{rwo} = \frac{\lambda_{\max}^{3+d_t-D_f} - \lambda_c^{3+d_t-D_f}}{\lambda_{\max}^{3+d_t-D_f} - \lambda_{\min}^{3+d_t-D_f}} = 1 - \left(\frac{\lambda_c}{\lambda_{\max}}\right)^{3+d_t-D_f} \quad (17)$$

Eq. (17) gives the final expression for liquid water relative permeability of GDL for the hydrophobicity case, where λ_c can be obtained in Eq. (15).

However, the carbon paper is treated to be waterproof in the actual application to PEMFCs. There may be two kinds of pores in a GDL, i.e. hydrophilic pores and hydrophobic pores coexisting. In this case, the water relative permeability is related to the fraction of the hydrophilic (or hydrophobic) pores to the total pores. f_{HI} (or f_{Ho}) and the value of water relative permeability can be obtained by averaging the relative permeability of the hydrophilicity case and the relative permeability of the hydrophobicity case [6]:

$$k_{rw} = f_{HI} k_{rwi} + (1 - f_{HI}) k_{rwo} \quad (18)$$

2.4. Determination of D_f

The area dimension D_f can be determined by the box-counting method [16]. This method is based on the image analysis of a unit cell or a sufficiently large cross-section of a sample along a plane normal to the flow direction. In this method, the cross-section under consideration is discretized using square boxes with size λ, and the number of boxes, $N(\lambda)$ required to completely cover the pore areas is counted. The area dimension, D_f can be determined by the value of the slope of a linear fit on a logarithmic plot of the cumulative number of pores versus the pore size λ.

Fig. 1 shows a micrograph (by SEM) of the GDL (TGP-H-120), where the carbon fibers and the pores formed by random packed fibers can be easily distinguished. Fig. 2 shows the data obtained by box-counting method with the length scale

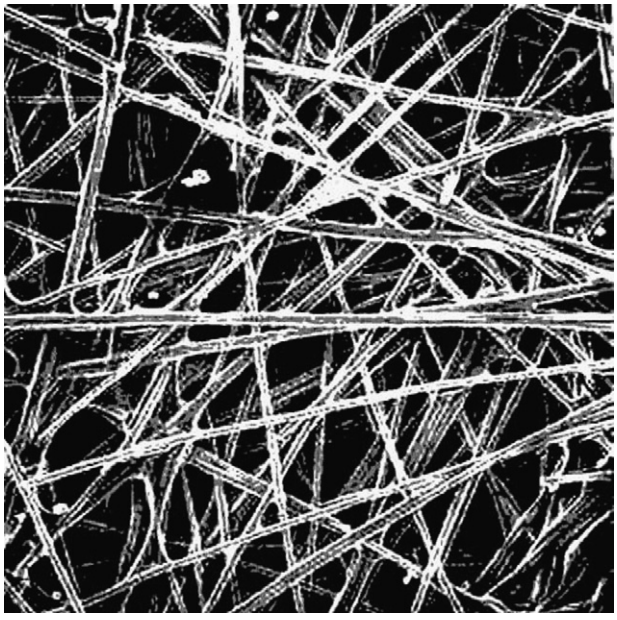

Fig. 1. A micrograph of TGP-H-120 (through-plane direction).

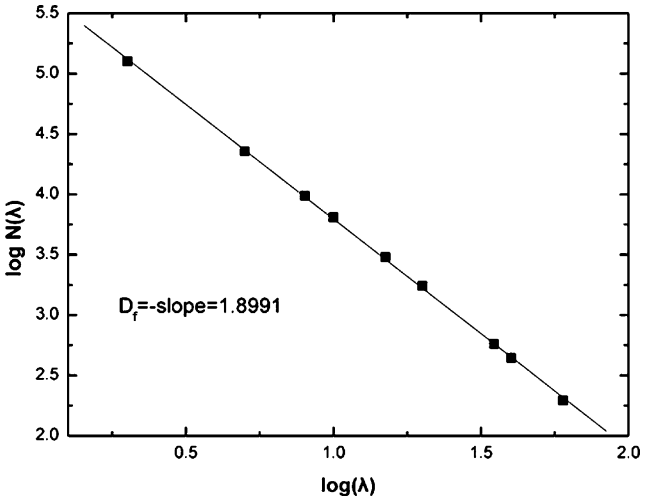

Fig. 2. Schematic illustration of the procedure for evaluation of the tortuosity dimension, D_f.

range from 2 to 60 pixels. The data follows a closely linear relationship on the logarithmic scale, and this confirms the statistical fractal nature of the microstructure of GDL. The value of area dimension is 1.8991 according to the slope of the data line.

2.5. Determination of tortuosity dimension, d_t

As mentioned previously, the tortuosity dimension represents the extent of convolution of the capillary pathways for water flowing through GDL. Since the tortuosity dimension pertains to the capillary pathways in the direction of the overall flow for the permeability evaluation, the microstructural images considered for the calculation of d_t are those of the GDL cross-section parallel to the flow direction (along the direction of thickness). Furthermore, since the tortuosity of the flow pathways results from the convolution of the boundaries of the porous regions as seen in a two-dimensional GDL cross-section, the tortuosity dimension may therefore be evaluated as the fractal dimension of the perimeter of the porous regions, which may also be obtained by the box-counting method mentioned above. Fig. 4 shows a log–log plot of $N(L)$ against L obtained by the box-mounting method for the micrograph of TGP-H-120 shown in Fig. 3. As expected, the number of boxes required to cover the perimeter decreases with increasing box size, and furthermore, the data points closely follow a straight line in the $\log(N(L))$–$\log(L)$ plot. The value of d_t is 1.2507 according to the slope of the linear fit in Fig. 4.

2.6. Determination of λ_{max}

The maximum pore size appeared in the permeability expression corresponding to the pore space formed between the carbon fibers in GDL. The spaces between carbon fibers are a function of the architectural parameters of the GDL, and the GDL considered in this study consists of random packed ideally equispaced aligned carbon fiber screens [17] shown in Fig. 5. For this structure, the maximum pore space may be considered to

Fig. 3. A micrograph of the GDL cross-section (TGP-H-120).

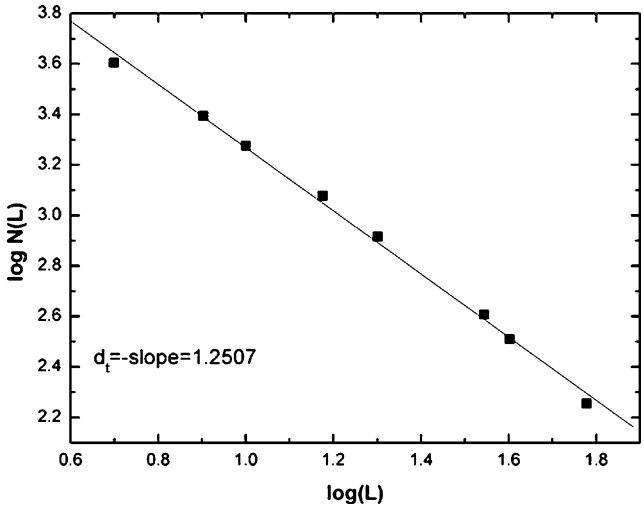

Fig. 4. Schematic illustration of the procedure for evaluation of the tortuosity dimension, d_t.

Fig. 5. An ideal carbon fiber screen.

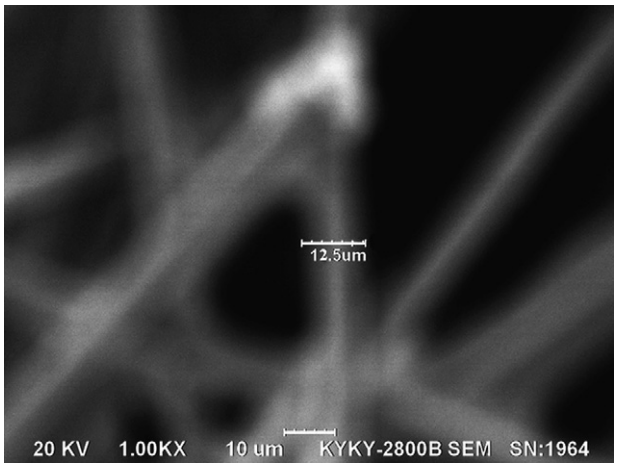

Fig. 6. A micrograph of the carbon fiber in GDL (TGP-H-120).

be resulted from a single ordered carbon fiber screen shown in Fig. 5. According to this equation

$$\varepsilon = \frac{l_s^2}{(l_s + d)^2} \tag{19}$$

Here, l_s is the length of the space, and d is the diameter of a carbon fiber. According to the micrograph shown in Fig. 6, it possess the value of 12.5 μm, and the porosity of TGP-H-120 is 0.78 (Toray Carbon Paper properties [10]), then the maximum pore size can be

$$\lambda_{max} = 2\sqrt{l_s^2/\pi} \tag{20}$$

3. Results and discussion

3.1. Predicted permeability

According to Eqs. (11), (19) and (20), the permeability of TGP-H-120 can be obtained. The permeability can also be obtained by the well-known Kozeny–Carman equation:

$$K = \frac{\varepsilon^3 d^2}{16 K_k (1-\varepsilon)^2} \tag{21}$$

For fibrous media, K_k is taken as 6 [17]. The predicted result by Kozeny–Carman equation and the fractal model in this study are compared with the experimental data by Williams et al. [1] (TGP-H-120, the value of permeability is 8.69E−12 m^2). The result of the present fractal model fits the experimental data well as shown in Fig. 7, so, the fractal model points out a new way to estimate the permeability of GDL in PEMFCs.

Fig. 8 shows the permeabilities for different tortuosity dimension, which reflect the extension of tortuosity in GDL. It can be seen that the permeability increases while d_t decreases. When $d_t = 1$, the permeability have the maximum value, which is consistent with the theory mentioned above, i.e. while $d_t = 1$, the capillaries are straight. It is advantageous for water flowing through. Fig. 9 shows the permeabilities for different area dimension D_f. It can be seen that the permeability increases with increase of D_f.

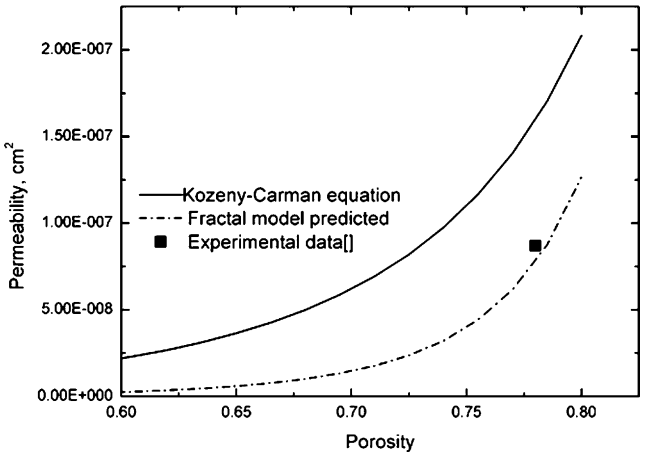

Fig. 7. A comparison between the fractal model predicting permeability and test data.

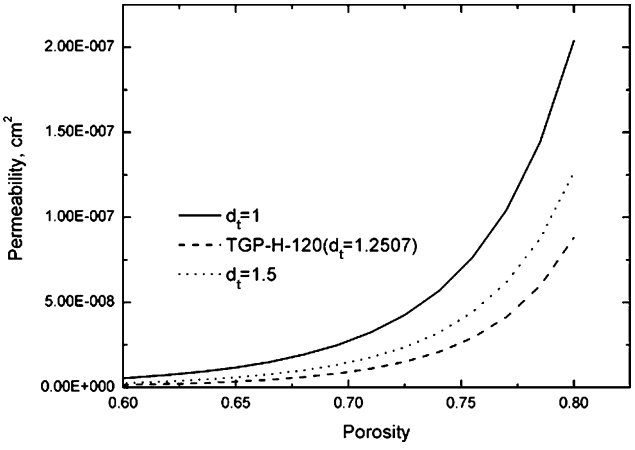

Fig. 8. Permeability as function of d_t.

3.2. Predicted water relative permeability

Fig. 10 shows the water relative permeabilities for the hydrophilicity case, hydrophobicity case, $f_{HI} = 0.3$, and 0.8. The results indicate that water relative permeability of the hydrophobicity case is much lager than that of the hydrophilicity case. And

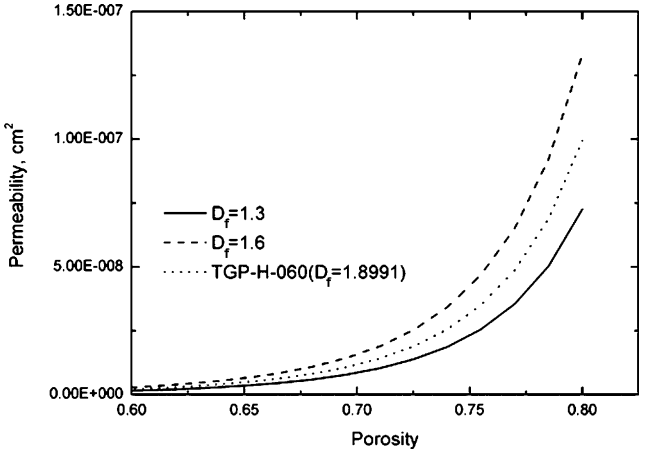

Fig. 9. Permeability as function of D_f.

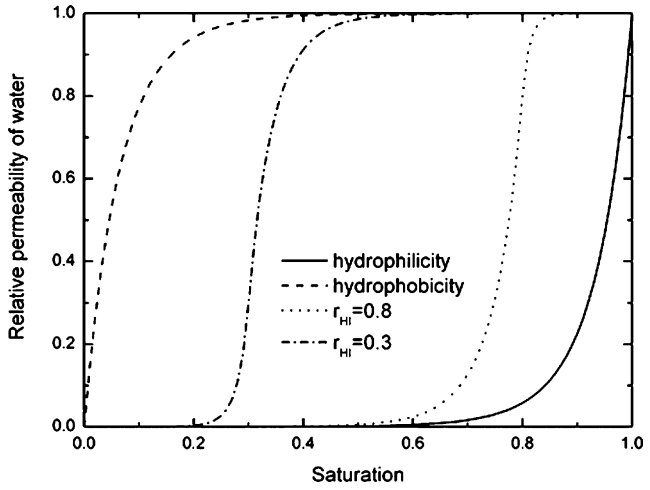

Fig. 10. Water relative permeabilities as functions of saturation for different hydrophilic pore fraction, $d_t = 1.2507$ (base case).

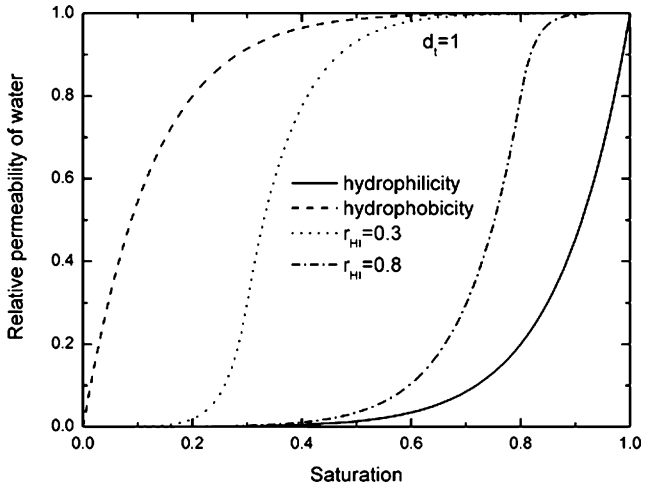

Fig. 11. Water relative permeabilities as functions of saturation for different hydrophilic pore fraction, $d_t = 1$.

water relative permeability of the hydrophobicity case increases quickly from 0 to nearly 1 with saturation changing from 0 to 0.4. But for the same range, the water relative permeability of the hydrophilicity case is really very low until the saturation comes to 0.6. It begins to increase quickly. The results also show that water relative permeability increases with the reducing of hydrophilic pore fraction.

Liquid water is produced in the cathode catalyst layer by the electrochemical reaction of PEMFCs. It must be efficiently removed otherwise it will cause "flooding" of the electrode which hinders the transport of the reactants. Liquid water removal from the cathode catalyst layer can be achieved in two ways: flow through the cathode GDL to the cathode gas channel; diffusion and convection through the membrane to the anode side. For the former case, according to the results shown above, hydrophobic carbon paper is preferred for its high water relative permeability. As for the case of diffusion and convection through the membrane, it will be better if the pressure of liquid water in the cathode catalyst layer side is high, due to the initial pressure needed for the hydrophobic pores. It also can be seen that hydrophobic carbon paper is preferred. The conclusion can be drawn that a hydrophobic GDL is better than a hydrophilic GDL in the view of liquid water removal on cathode side of PEMFCs.

For anode side, liquid water accumulation in the anode side is determined by the transport of water in the membrane, which is mainly via diffusion, convection and electro-osmotic drag. Two situations should be considered: one is the transport direction of water from anode to cathode, the other is the transport direction of water from cathode to anode. If liquid water transports from the anode to the cathode, it may cause water-depletion on the anode side. So it is necessary to maintain a certain quantity of water on the anode side. From this point of view, a hydrophilic GDL is suitable for its low water relative permeability. However, if liquid water transports from the cathode to the anode, there may be an accumulation of liquid water on the anode side, so a hydrophobic GDL is preferred.

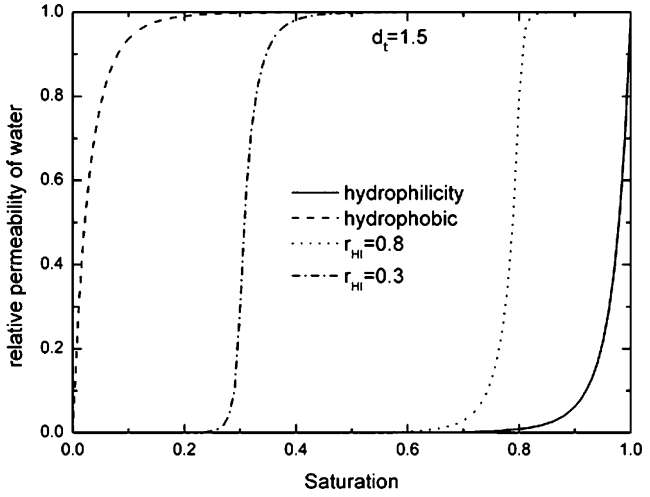

Fig. 12. Water relative permeabilities as functions of saturation for different hydrophilic pore fraction, $d_t = 1.5$.

Figs. 11 and 12 show the water relative permeabilities for different tortuosity dimensions. The results show that the water relative permeability of the hydrophilicity case decreases with increase of the tortuosity dimension, and the water relative permeability of the hydrophobicity case increases with increase of tortuosity dimension.

4. Conclusion

In this study, a fractal model is developed to predict the permeability and liquid water relative permeability of the GDL (TGP-H-120 carbon) in PEMFCs for the hydrophilicity case and the hydrophobicity case. Area dimension, tortuosity dimension, maximum pore size, thickness of GDL, and saturation as well as the hydrophilic pore fraction in the GDL are involved in this model. The area dimension and tortuosity dimensions are obtained by the box-counting method based on the micrographs (in-plane and through-plane) of TGP-H-120. The model

is validated by the comparison between predicted results and experimental data. The results indicate:

1. The permeability of the GDL increases with the decrease of the tortuosity dimension or the increase of the area dimension.
2. The water relative permeability of the hydrophobicity case is much higher than that of the hydrophilicity case.
3. To effectively remove the water on the cathode side of PEMFCs, hydrophobic carbon paper is better than hydrophilic carbon paper. As for the anode side, if water flows from the cathode to the anode, a hydrophobic carbon paper is preferred, otherwise, hydrophilic carbon paper should be applied.
4. Water relative permeability increases with increase of the tortuosity dimension for the hydrophobicity case but decreases for the hydrophilicity case.

References

[1] M.V. Williams, E. Begg, L. Bonville, H. Russell Kunz, J.M. Fenton, J. Electrochem. Soc. 151 (2004) A1173–A1180.
[2] M. Prasanna, H.Y. Ha, E.A. Cho, S.A. Hong, I.H. Oh, J. Power Sources 131 (2004) 147–154.
[3] M.V. Williams, H. Russell Kunz, J.M. Fenton, J. Electrochem. Soc. 151 (2004) A1617–A1627.
[4] C. Lim, C.Y. Wang, Electrochim. Acta 49 (2004) 4149–4156.
[5] L.R. Jordan, A.K. Shukla, T. Behrsing, N.R. Avery, B.C. Muddle, M. Forsyth, J. Appl. Electrochem. 30 (2000) 641–646.
[6] A.Z. Weber, R.M. Darling, J. Newman, J. Electrochem. Soc. 151 (2004) A1715–A1727.
[7] B.B. Mandelbrot, The Fractal Geometry of Nature, W.H. Freeman, New York, 1983.
[8] J. Feder, Fractals, Plenum Press, New York, 1988.
[9] R. Pitchumani, S.C. Yao, Trans. ASME J. Heat Transfer 113 (1991) 788–796.
[10] M. Mathias, J. Roth, J. Fleming, W. Lehnert, Handbook of Fuel Cells—Fundamentals, Technology and Applications, John Wiley and Sons, Ltd., 2003 (Chapter 46).
[11] R. Pitchumani, B. Ramakrishnan, Int. J. Heat Mass Transfer 42 (1999) 2219–2232.
[12] S.W. Wheatcraft, S.W. Tyler, Water Resour. Res. 24 (1988) 566–578.
[13] A. Majumdar, B. Bhushan, J. Tribol. 112 (1990) 205–216.
[14] M.M. Denn, Process Fluid Mechanics, Prentice-Hall, Englewood Cliff, NJ, 1980.
[15] http://www.torayca.com/properties/en/images/report_eng09_2.html.
[16] J. Feder, A. Aharony, Fractals in Physics, North-Holland, Amsterdam, 1989.
[17] M. Kaviany, Principles of Heat Transfer in Porous Media, 2nd ed., Springer, New York, 1999.